

Fig. 1 Schematic cross-section through propagation direction of coplanar transmission lines

## Coplanar waveguides on dielectric membranes micromachined on a GaAs substrate

P. Salzenstein, O. Dupuis, M. Héjal, E. Lheurette, O. Vanbésien, P. Mounaix and D. Lippens

Indexing terms: Coplanar waveguides, Transmission lines

GaAs micromachining technology was used for fabricating coplanar transmission lines on  $\text{Si}_3\text{N}_4$  and polyimide membranes deposited on GaAs substrates. On-wafer measurements of scattering parameters up to 75GHz for several line configurations show a constant phase velocity of  $2.9 \cdot 10^8$  m/s and a predominance of metallic losses with a square root frequency dependence.

**Introduction:** High speed transmission lines are of prime importance for a variety of applications, notably those concerning monolithic microwave integrated circuits (MMICs). Until now, most of the transmission lines were fabricated in a coplanar configuration on relatively thick substrates. However, there are drawbacks to the use of thick substrates. Therefore, for a frequency around 100GHz, modal dispersion occurs along with a decrease in the phase velocity owing to the preferential confinement of the guided mode to the substrate material. In addition to this dispersion issue, it has been shown that high frequency losses are also dominated by radiation into the substrate with a rapid increase in the attenuation coefficient with a near cubic frequency dependence [1]. Such a dispersion and loss increase are serious drawbacks for many applications at millimetre and submillimetre wavelengths. A possible way to overcome these limitations is to shrink the substrate thickness or to use a substrate-free propagation structure. On this basis, several techniques have shown promise, notably dielectric membranes usually a tri-layer  $\text{SiO}_2/\text{Si}_3\text{N}_4/\text{SiO}_2$  deposited on silicon substrate [2] or silicon membranes [3]. In this Letter, we investigate the solution of a dielectric membrane ( $\text{Si}_3\text{N}_4$  or polyimide) micromachined on a GaAs substrate which supports a coplanar waveguide (CPW). Since most of the solid state devices operating at very high frequency are fabricated in the GaAs material system, it is expected that such a scheme will provide greater functionality in the design of monolithic circuits including active and passive components, and hence a better integration.

**Design and fabrication:** Fig. 1 shows a schematic cross-section through the propagation direction of the transmission lines we fabricated. To measure the complex propagation constant  $\gamma = \alpha + j\beta$  where  $\alpha$  and  $\beta$  are the attenuation and phase constants, respectively, the mask set includes several line structures with different lengths ( $L = 3.5, 7$  and  $13\text{mm}$ ). In addition, several geometries were investigated by varying the characteristic impedance of transmission lines supported by a membrane. In a first approach for this design, we used the analytical formula of [4] in

order to know in what extent the characteristic impedance  $Z_c$  varies when the substrate thickness of the substrate is dramatically shrunk. Subsequently, we used a full-wave analysis for determining more accurately [5] the geometry of a CPW supported by a membrane for three values of characteristic impedances  $Z_c = 50, 75$  and  $100\Omega$ . In practice, the dimensions chosen are the following: for  $Z_c = 50\Omega$ ,  $w = 550\mu\text{m}$ ,  $s = 10\mu\text{m}$ ; for  $Z_c = 75\Omega$ ,  $w = 300\mu\text{m}$ ,  $s = 27\mu\text{m}$  and for  $Z_c = 100\Omega$ ,  $w = 300\mu\text{m}$ ,  $s = 75\mu\text{m}$ .

Basically, the process flow is divided into two steps involving a front-side processing (dielectric and metal deposition) and a back-side processing (bulk machining of a cavity) which is performed in a last stage hence reducing the risk of deterioration of samples. On a semi-insulating  $400\mu\text{m}$  GaAs substrate we first deposited a  $\text{Si}_3\text{N}_4$  layer using plasma enhanced chemical vapour deposition (PECVD), or a polyimide film by spin coating, followed by a post-bake. Typically the thickness of this dielectric layer is between 1 and  $2\mu\text{m}$ . Under these conditions, the stress can be controlled and we obtained films usually with a tensile stress. For the metal deposition of coplanar lines, two techniques can be used: either the etch-masking process or the lift-off process. In this Letter we used the latter process for aspect ratio considerations. Indeed, as seen above, the narrowest slot has a width  $s$  of  $10\mu\text{m}$ , whereas the line length ( $L$ ) is of several millimetres. Therefore, we first deposited a  $\text{Ti } 200\text{\AA}/\text{Au } 200\text{\AA}$  film by evaporation, followed by electroplating of a thick gold layer ( $t \sim 2\mu\text{m}$ ). This metal layer uniformly deposited was subsequently patterned and then etched using gold and titanium etchants, paying attention to the resist and metal profiles. After completing this metallisation, the wafer was then patterned on the back-side in order to entirely remove the GaAs material underneath the area defining the membrane. This etch for micromachining of the cavity was made by wet chemical etching using  $\text{H}_2\text{SO}_4:1/\text{H}_2\text{O}_2:8/\text{H}_2\text{O}:1$  and photoresist as a mask. These concentrations offer the advantage of a high etching rate (typically  $15\mu\text{m min}^{-1}$ ) and a high selectivity against photoresists and dielectric layers. However, the etching was found to be highly anisotropic with a pronounced tilted profile along the (011) section. As a consequence, it was decided to take advantage of such an etching profile to provide a tapered transition between the probing region on the semi-insulating substrate and the substrate-free region onto the membrane. This also means that the mask opening on the back-side should be closely adjusted to fit the length  $L$  of the transmission lines. This step was found to be the most critical, requiring careful alignment using double-side photolithography equipment.

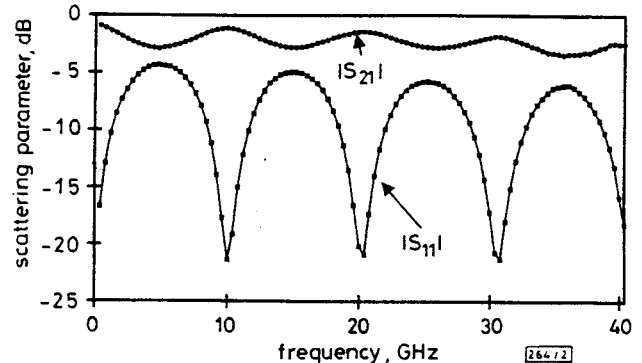


Fig. 2 Measured  $S_{11}$  and  $S_{21}$  for a  $100\Omega$  transmission line with length of  $13\text{mm}$  supported by a polyamide membrane

$50\Omega$  access region

P. Salzenstein, O. Dupuis, M. H elal, E. Lheurette, O. Vanb esien, P. Mounaix and D. Lippens (Institut d'Electronique et de Micro electronique du Nord, Universit  des Sciences et Technologies de Lille, Avenue Poincar  BP 69, 59652 Villeneuve d'Ascq Cedex, France)

References

- 1 FRANKEL, M.Y., GUPTA, S., VALDMANIS, J.A. and MOUROU, G.A.: 'Terahertz attenuation and dispersion characteristics of coplanar transmission lines'. *IEEE Trans. Microw. Theory Tech.*, 1991, **39**, (6), pp. 910-916
- 2 WELLER, M.T., KATEHI, L.P.B. and REBEIZ, G.M.G.: 'High performance microshield line components'. *IEEE Trans. Microw. Theory Tech.*, 1995, **43**, (3), pp. 534-543
- 3 FRANKEL, M.Y., VOELKER, R.H. and HILFIKER, J.N.: 'Coplanar transmission lines on thin substrates for high speed low loss propagation'. *IEEE Trans. Microw. Theory Tech.*, 1994, **42**, (3), pp. 396-401
- 4 GHIONE, G. and NALDI, C.: 'Analytical formulas for coplanar lines in hybrid and monolithic MICs'. *Electron. Lett.*, 1984, **20**, (4), pp. 179-181
- 5 H ELAL, M., LEGIER, J.F., PRIBETICH, P. and KENNIS, P.: 'Analysis of planar transmission lines and microshield lines with arbitrary metalization cross sections using finite elements methods'. *IEEE MTT Symp.*, 1994, Paper WE3F-31, pp. 1041-1044
- 6 BIANCO, B. and PARODI, M.: 'Determination of the propagation constant of uniform microstrip lines'. *Alta Freq.*, 1976, **2**, pp. 109-110

**RF measurements:** For frequency evaluation of the performance of the CPW, we measured the scattering parameters using RF probes and network analysers operating either between 1 and 40GHz or between 50 and 75GHz. Fig. 2 shows the variations of the magnitudes of reflection coefficient  $S_{11}$  ( $S_{22} = S_{11}$ ) and transmission coefficient  $S_{12}$  ( $S_{21} = S_{12}$ ) for a coplanar waveguide on a membrane with a characteristic impedance  $Z_c = 100\Omega$  and a length  $L = 13\text{mm}$ . Owing to the impedance mismatch between the feeding lines of  $50\Omega$  characteristic impedance and the transmission lines supported by a membrane, well behaved resonance effects can be noticed in the frequency dependence of scattering parameters. These resonances are a direct consequence of the matching of the wavelength of CPW on a membrane and of the distance over which the electromagnetic wave is bouncing back and forth, which includes  $L$  and the tapered access. In the case of a strong mismatch, where the line section on the membrane behaves as a resonator, a first estimate of the phase velocity  $v_\phi$  can be made from resonance conditions ( $f_r = nv_\phi/2L$ , where integer  $n$  is the resonance index). The slow decrease in the magnitude of  $S_{ij}$  at increasing frequency is caused by intrinsic losses increasing with frequency, which attenuate both the transmitted and reflected waves. At this stage, in order to get more insight into the loss variation as a function of frequency, and the dispersion characteristics, we analysed the experimental data using the method proposed by Bianco and Parodi in [6]. By means of this transmission and reflection technique, which compares two lines of different lengths, it is possible to derive the complex propagation constant  $\gamma$  from  $S_{ij}$  measurements. Fig. 3 shows the frequency dependence of attenuation constant  $\alpha$  plotted in log-log scales, along with the phase constant  $\beta$  given in the inset, calculated using this procedure. For the former, a square root behaviour against frequency is noted, whereas no dispersion can be seen in the  $\beta(f)$  plot which exhibits a linear variation against frequency.

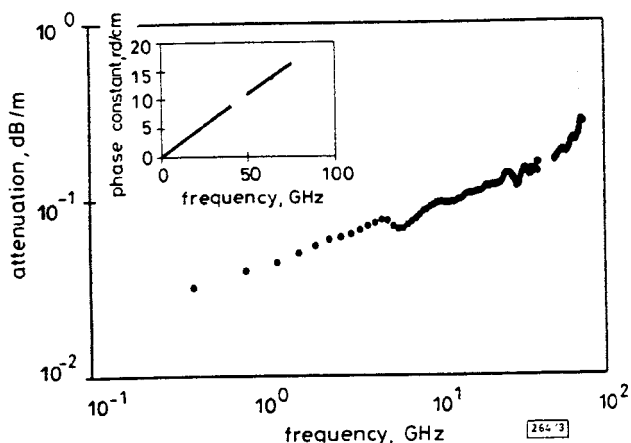


Fig. 3 Complex propagation constant against frequency for transmission line deposited on polyimide

**Discussion and conclusion:** From the  $\beta(f)$  characteristic, the effective dielectric constant  $\epsilon_{eff} = \beta^2/(\omega^2\mu_0\epsilon_0)$ , where  $\epsilon_0$  and  $\mu_0$  are the permittivity and permeability of vacuum, respectively, can be deduced. From Fig. 3 we thus calculated  $\epsilon_{eff} = 1.08$  which corresponds to a phase velocity  $v_\phi = c/\sqrt{\epsilon_{eff}} = 2.9 \cdot 10^8 \text{ms}^{-1}$ . This value of  $v_\phi$ , which is very close to the value of the velocity of light  $c$ , is significantly higher than those found for silicon membranes with a thickness of  $8\mu\text{m}$  [3]. This improvement can be explained by the use of an ultra-thin membrane with lower relative permittivity, notably for polyimide films ( $\epsilon_r = 2.9$ ). For the frequency range investigated it can be seen that the attenuation is dominated by metallic losses, in view of the square root frequency dependence which is characteristic of skin effects in conductors. As for conventional CPWs, the loss level will depend on the geometry, notably of conductor cross-sections, which can be optimised with the use of membranes, but also on the processing techniques with implications on the resistivity of the metal film and on its roughness.

**Acknowledgments:** The authors would like to thank P. Legry and S. Lepilliet for technical assistance.